Supporting information

Luminescence turn-on sensor for the selective detections of trace water and methanol based on a Zn(II) coordination polymer with 2,5-dihydroxyterephthalate

Jitti Suebphanpho[a] and Jaursup Boonmak[a]*

[a]*Materials Chemistry Research Center, Department of Chemistry, Faculty of Science, Khon Kaen University, Khon Kaen 40002, Thailand.*

**E-mail: jaursup@kku.ac.th*

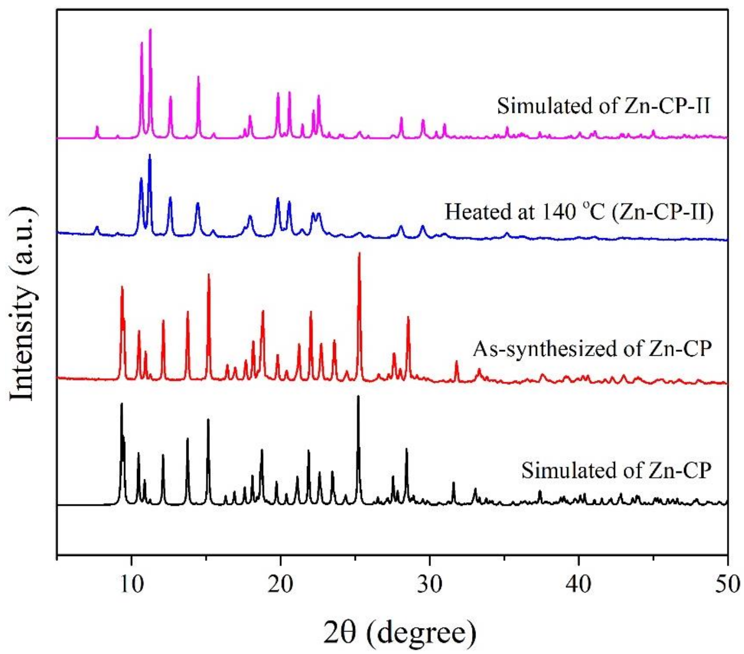

Fig. S1 PXRD patterns of as-synthesized samples compared with the simulated patterns **Zn-CP** and **Zn-CP-II**.

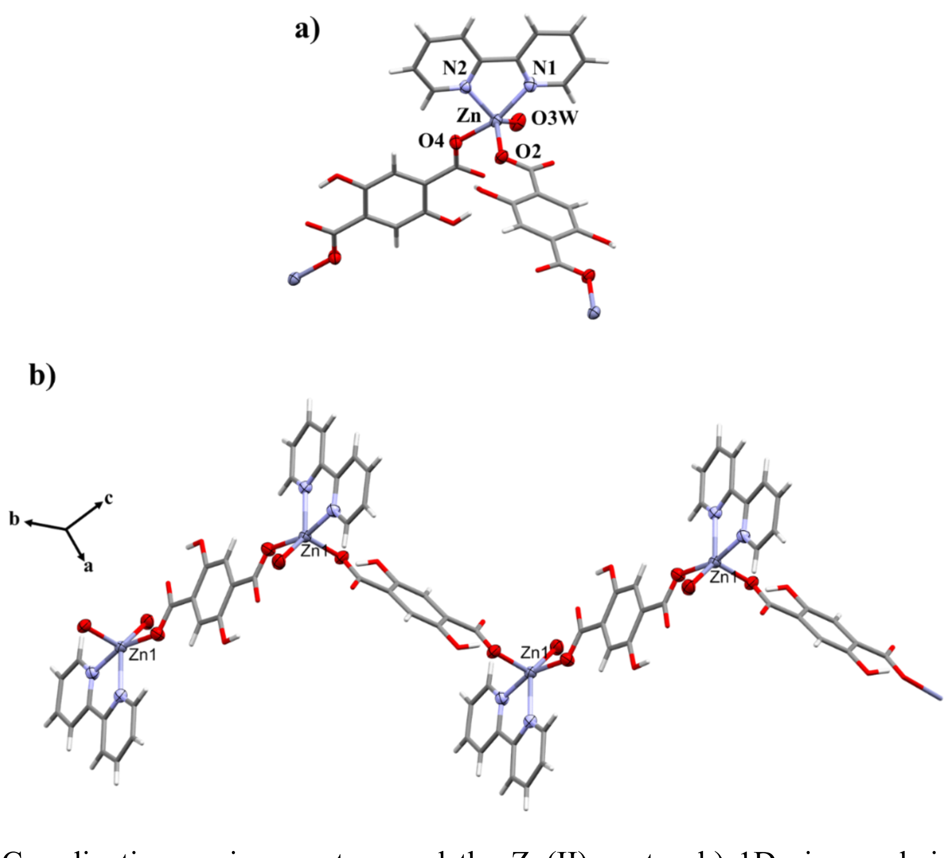

Fig. S2 a) Coordination environment around the Zn(II) center. b) 1D zigzag chain of **Zn-CP** through linker H_2dhtp^{2-} ligand.

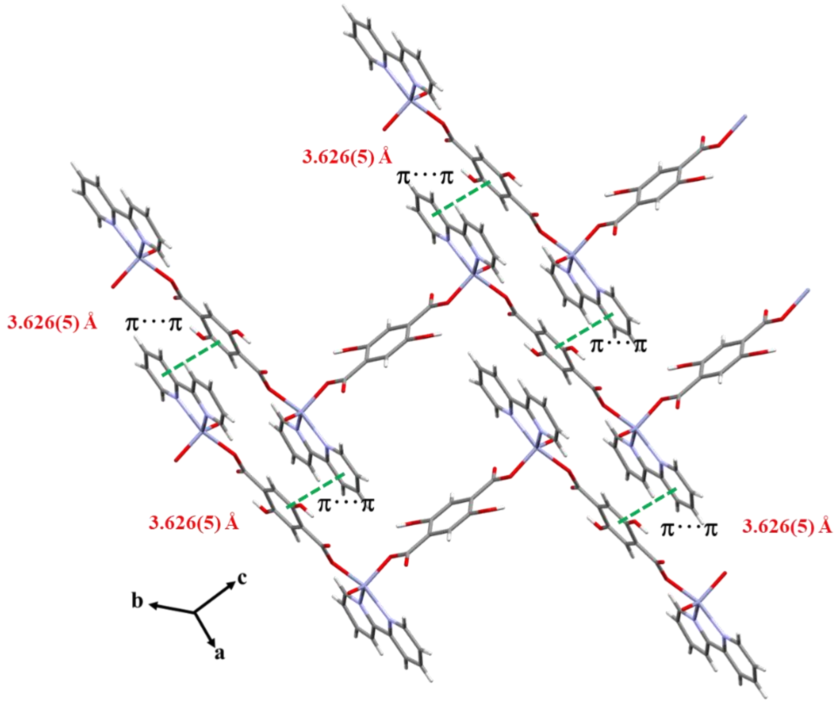

Fig. S3 2D layer of **Zn-CP** via π-π interaction along the *c*-axis between aromatic and pyridine rings of H_2dhtp^{2-} and chelating 2,2'-bpy ligands.

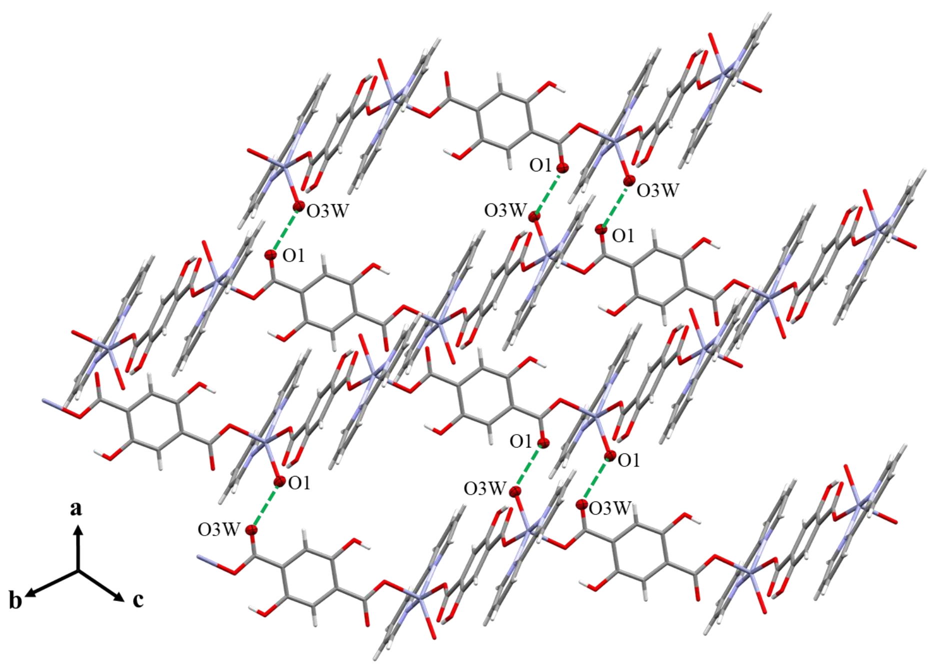

Fig. S4 The packing structure of **Zn-CP** presents a 3D supramolecular framework via hydrogen bonding between coordinated water molecules and uncoordinated oxygen atoms from carboxyl groups along the *b*-axis.

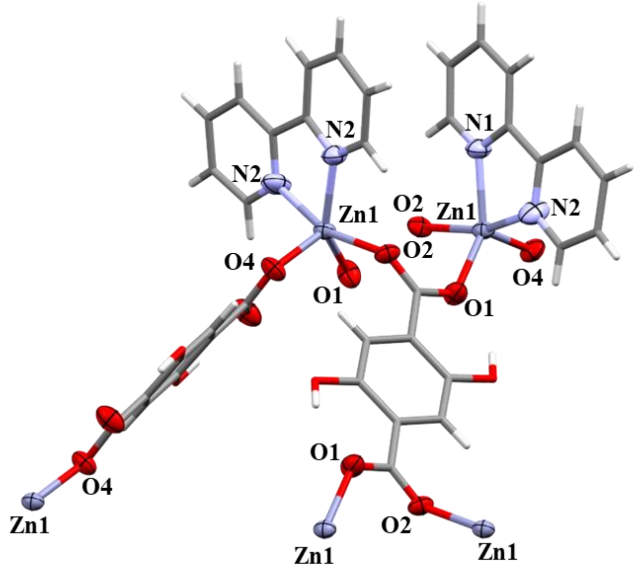

Fig. S5 Coordination environment around the Zn(II) center of **Zn-CP-II**.

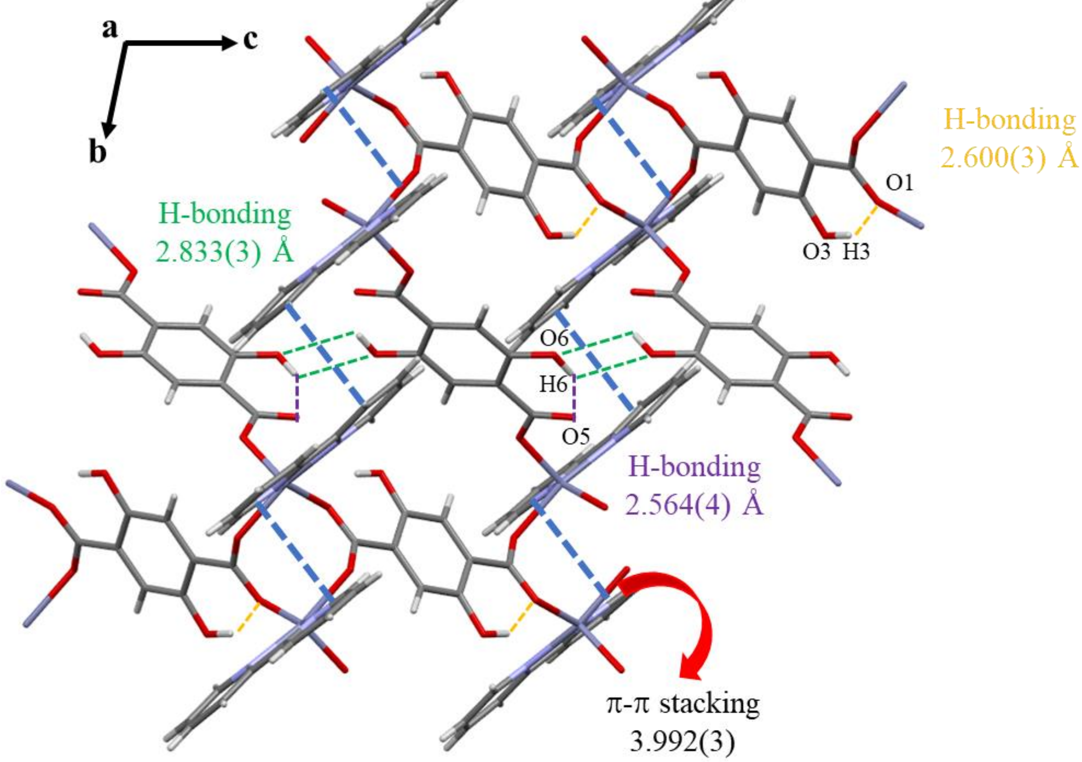

Fig. S6 2D layer and intramolecular interaction (π-π stacking between pyridyl rings of 2,2'-bpy and H-bonding between hydroxy groups of H_2dhtp^{2-}) of **Zn-CP-II**.

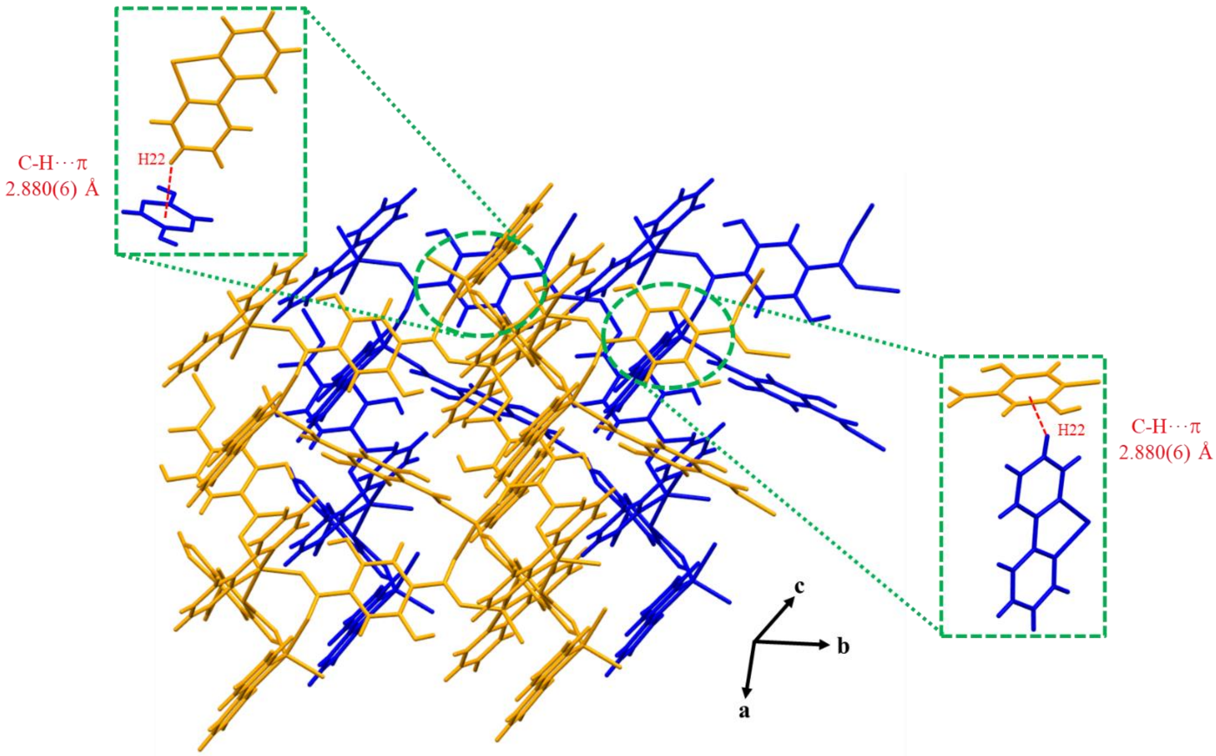

Fig. S7 3D supramolecular framework via C-H···π interaction (red dashed line) of **Zn-CP-II**.

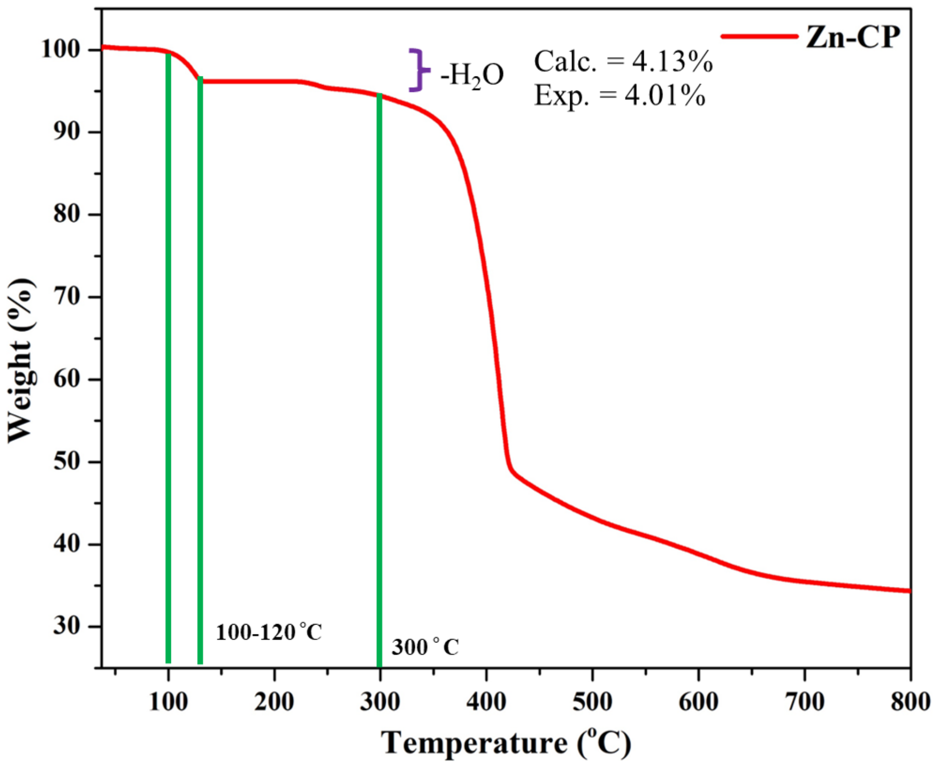

Fig. S8 The thermogram of **Zn-CP**.

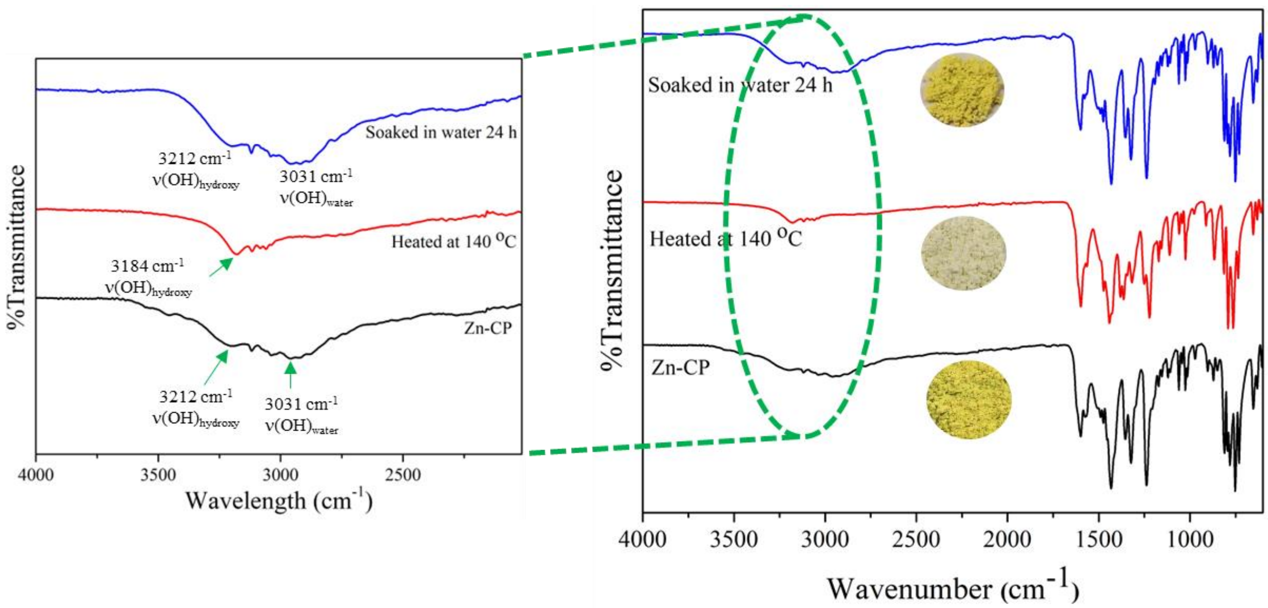

Fig. S9 FTIR spectra before and after dehydration and rehydration processes of **Zn-CP**.

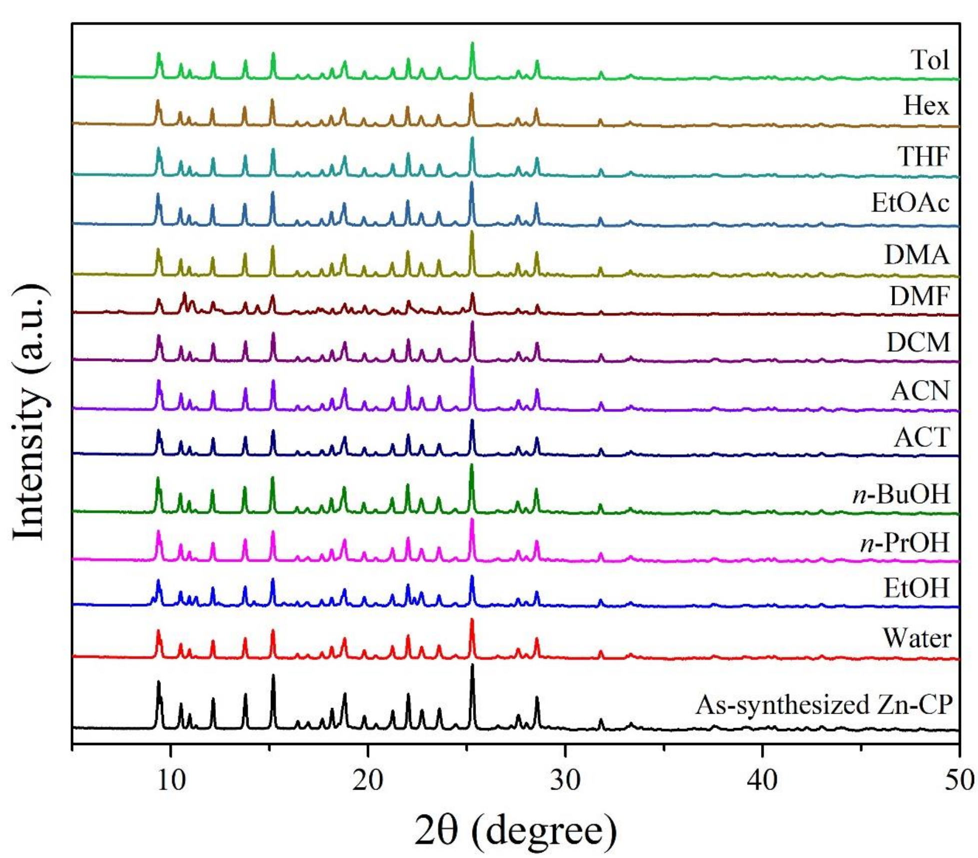

Fig. S10 PXRD patterns of **Zn-CP** after soaking in common organic solvents for 24 h at room temperature.

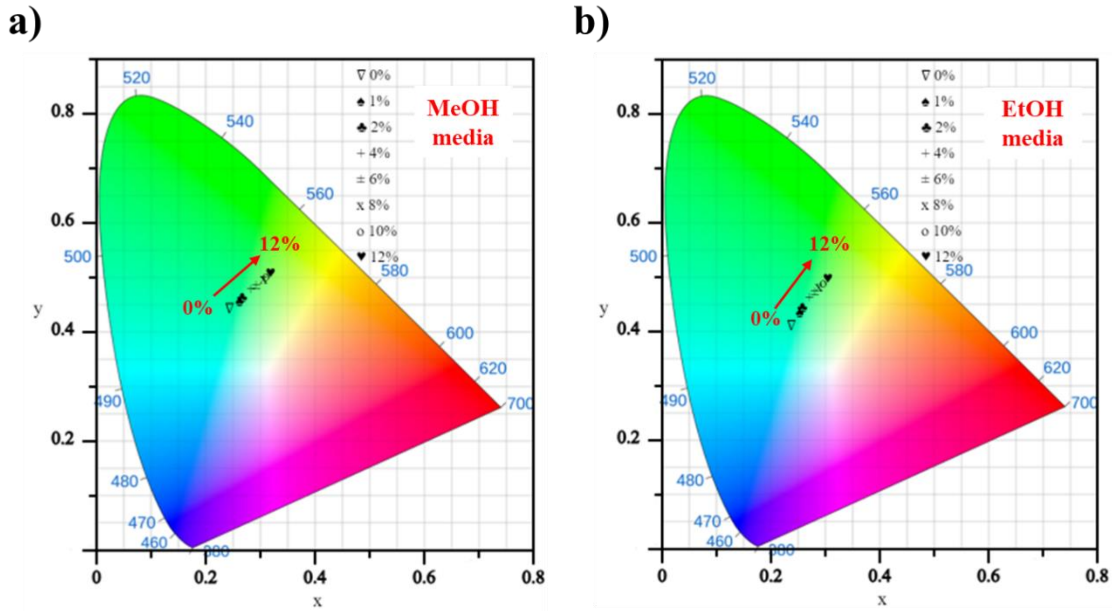

Fig. S11 CIE chromaticity diagrams for **Zn-CP** probe before and after adding different contents of water in dry methanol a) and b) dry ethanol.

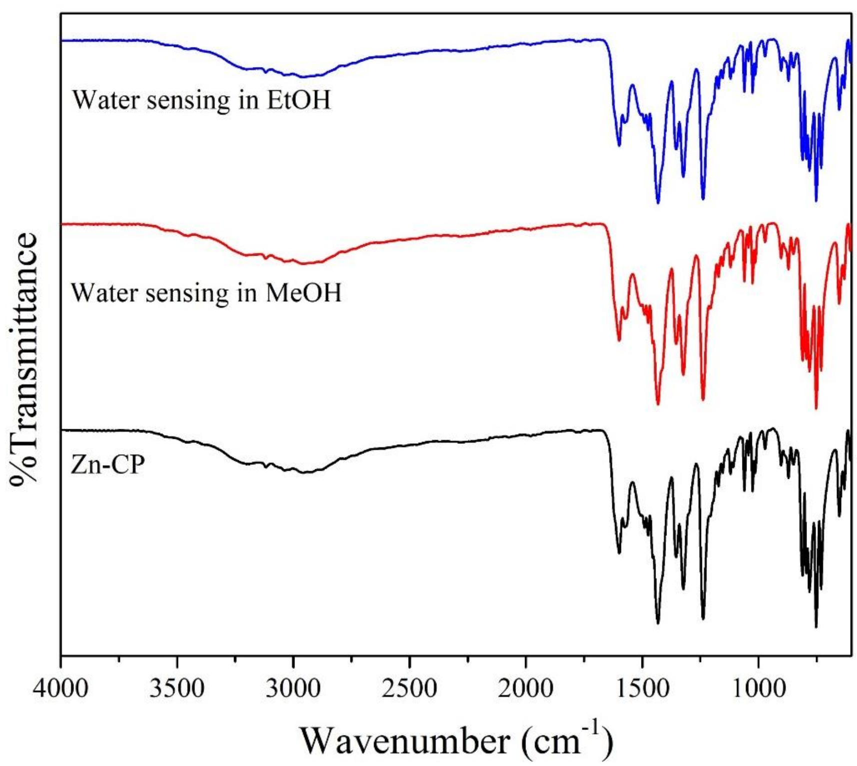

Fig. S12 FTIR spectra of **Zn-CP** before and after water sensing in dry methanol and dry ethanol.

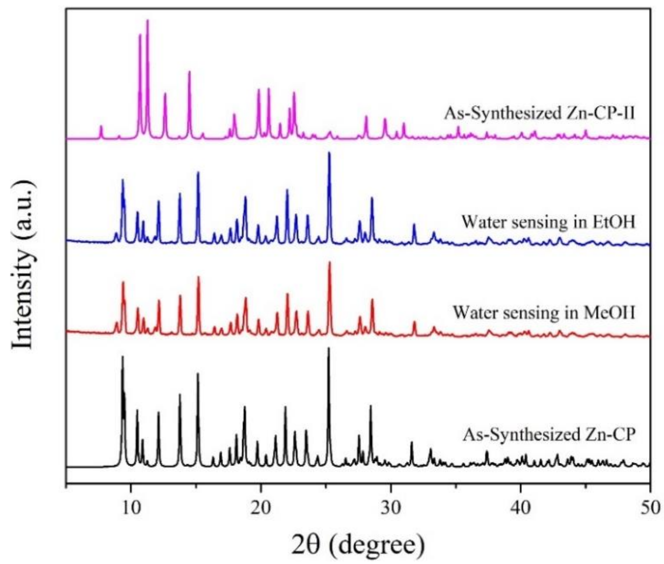

Fig. S13 PXRD patterns of **Zn-CP** before and after water sensing in dry methanol and dry ethanol.

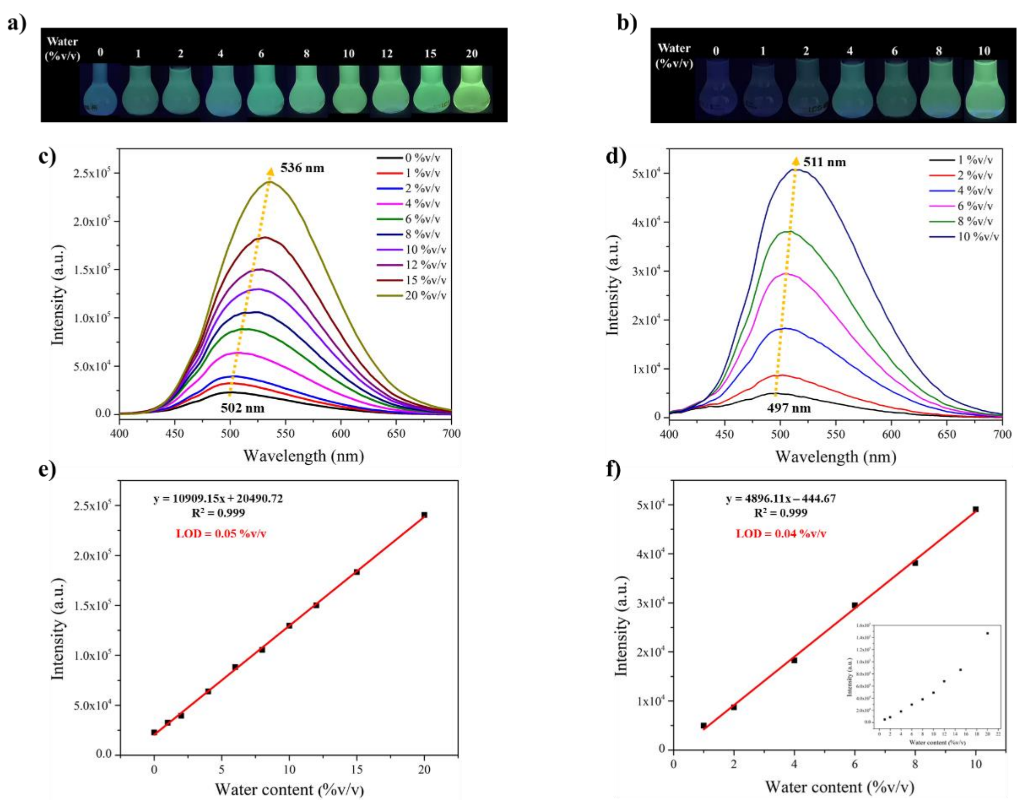

Fig. S14 Photographic images of the suspension of **Zn-CP-II** in a) dry methanol and b) dry ethanol with different water levels (0−12%). c) and d) Luminescence emission spectra of **Zn-CP-II** probe upon adding different contents of water in dry methanol and dry ethanol, respectively. e) and f) Linear relationship between the emission wavelength or luminescence intensity and water contents of **Zn-CP-II** probe in methanol and ethanol respectively. The inset show fluorescence intensity upon incremental addition of water 0-20%v/v.

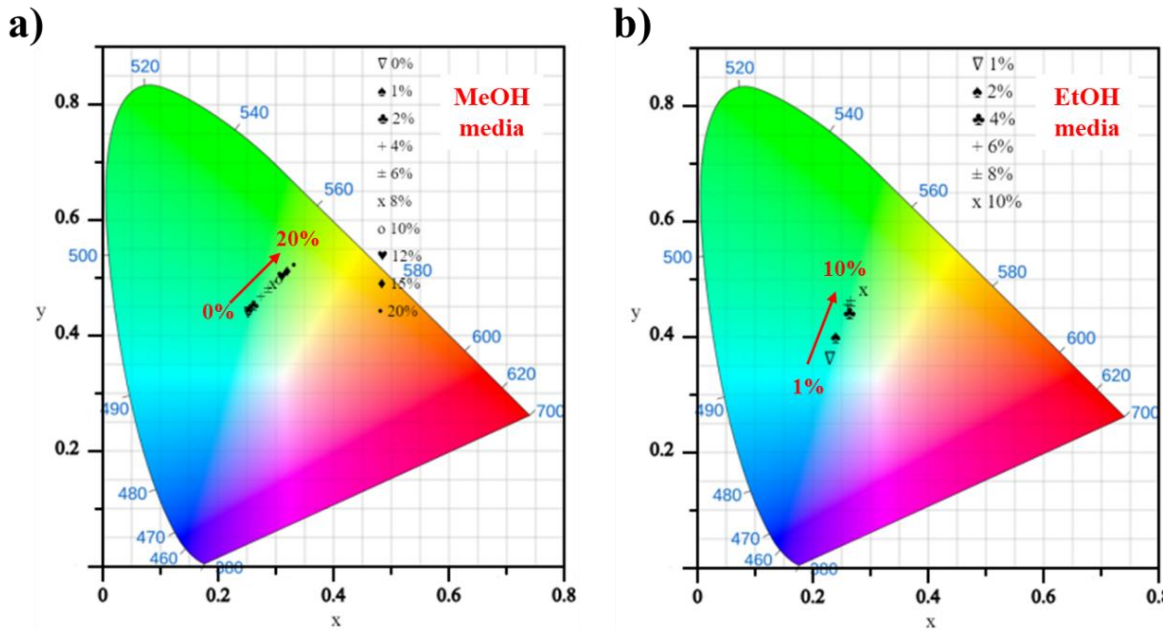

Fig. S15 CIE chromaticity diagrams for **Zn-CP-II** probe before and after adding different contents of water in dry methanol a) and b) dry ethanol.

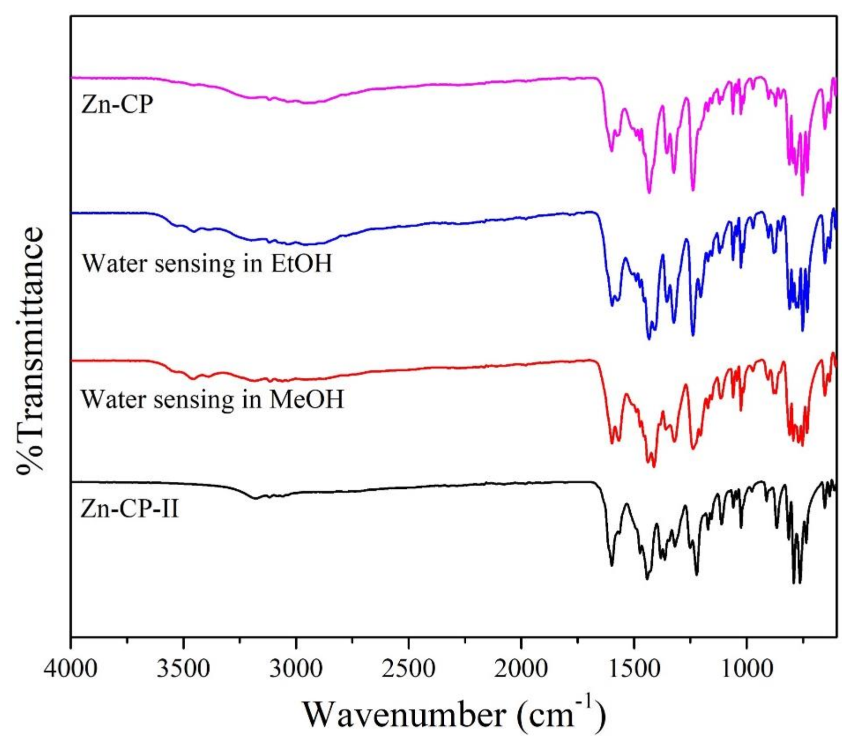

Fig. S16 FTIR spectra of **Zn-CP-II** before and after water sensing in dry methanol and dry ethanol.

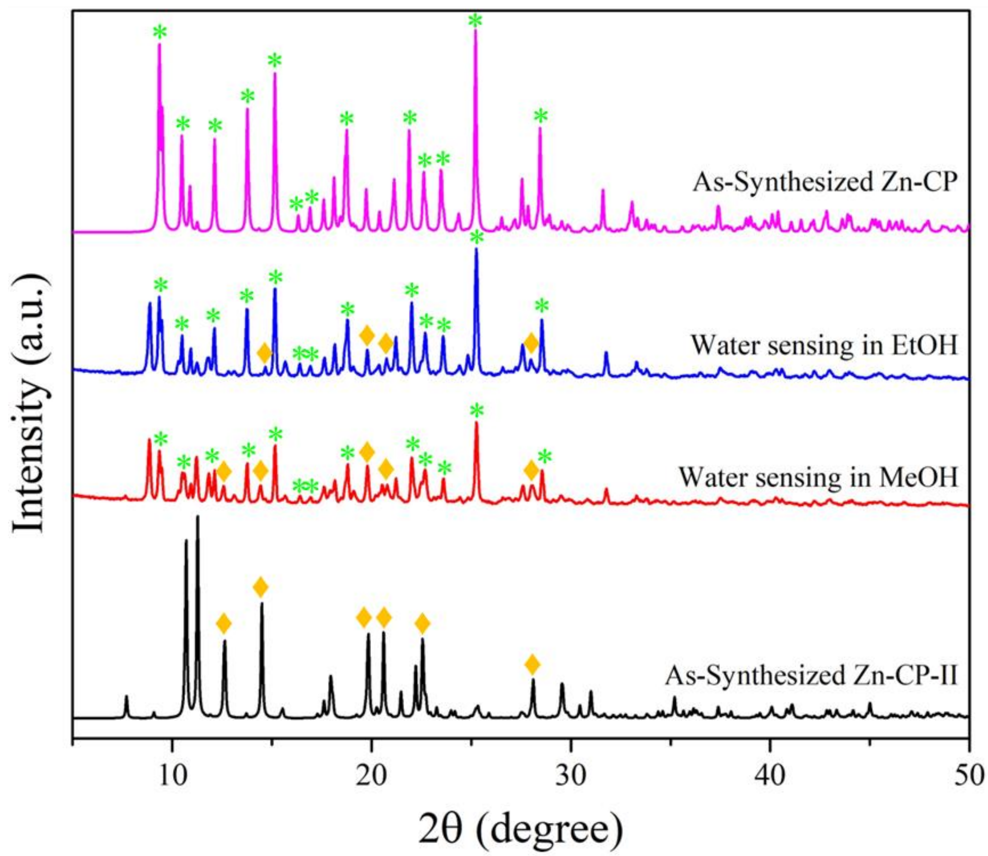

Fig. S17 PXRD patterns of **Zn-CP-II** before and after water sensing in dry methanol and dry ethanol. The green star and orange diamond symbols represent characteristic diffraction peaks for **Zn-CP** and **Zn-CP-II**, respectively.

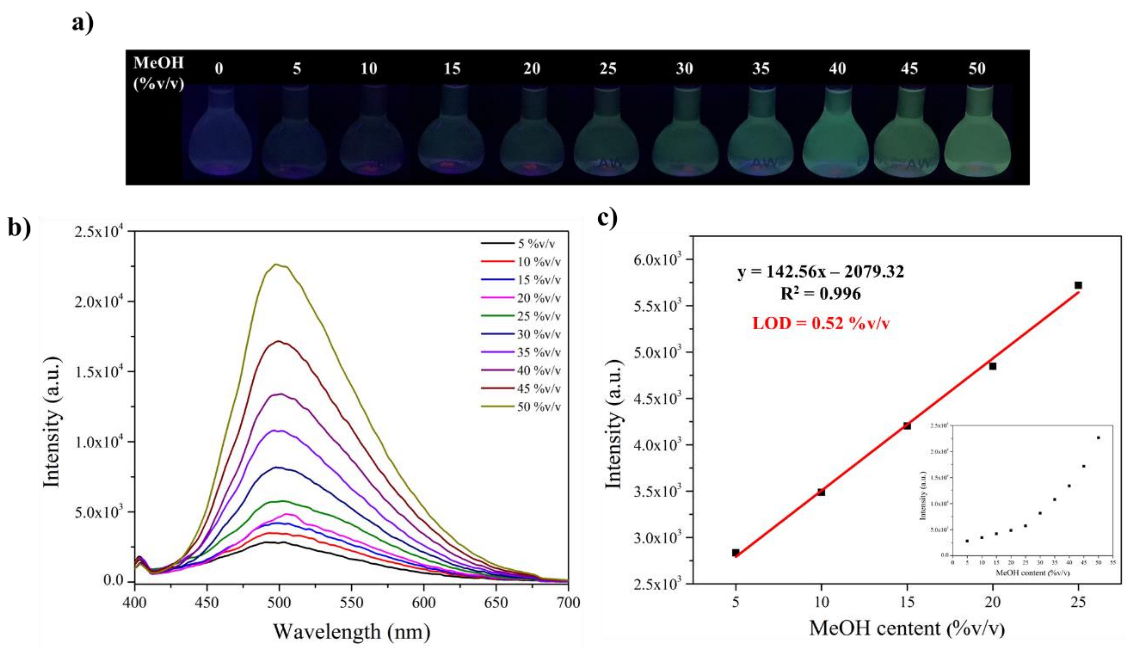

Fig. S18 a) Photographic images of the suspension of **Zn-CP** in dry *n*-propanol with different methanol levels (0-50 %v/v). b) Luminescence emission spectra of **Zn-CP** probe upon adding different content of methanol in dry *n*-propanol. c) Linear relationship between the luminescence intensity and methanol content of **Zn-CP**.

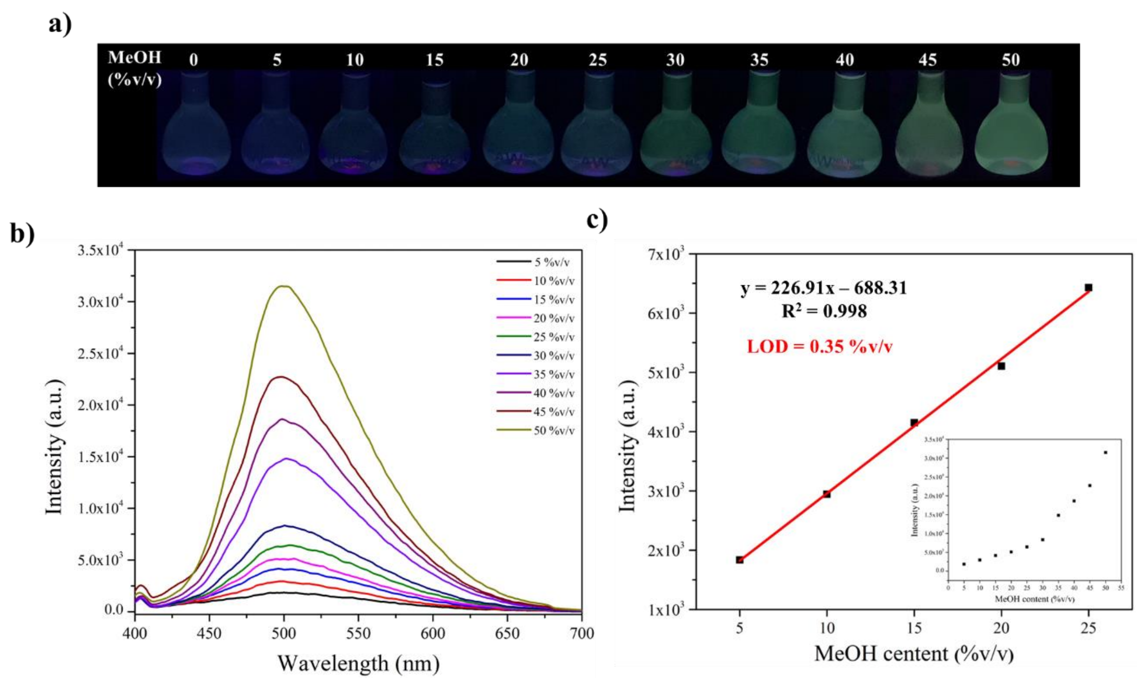

Fig. S19 a) Photographic images of the suspension of **Zn-CP** in dry *n*-butanol with different methanol levels (0-50 %v/v). b) Luminescence emission spectra of **Zn-CP** probe upon adding different content of methanol in dry *n*-butanol. c) Linear relationship between the luminescence intensity and methanol content of **Zn-CP**.

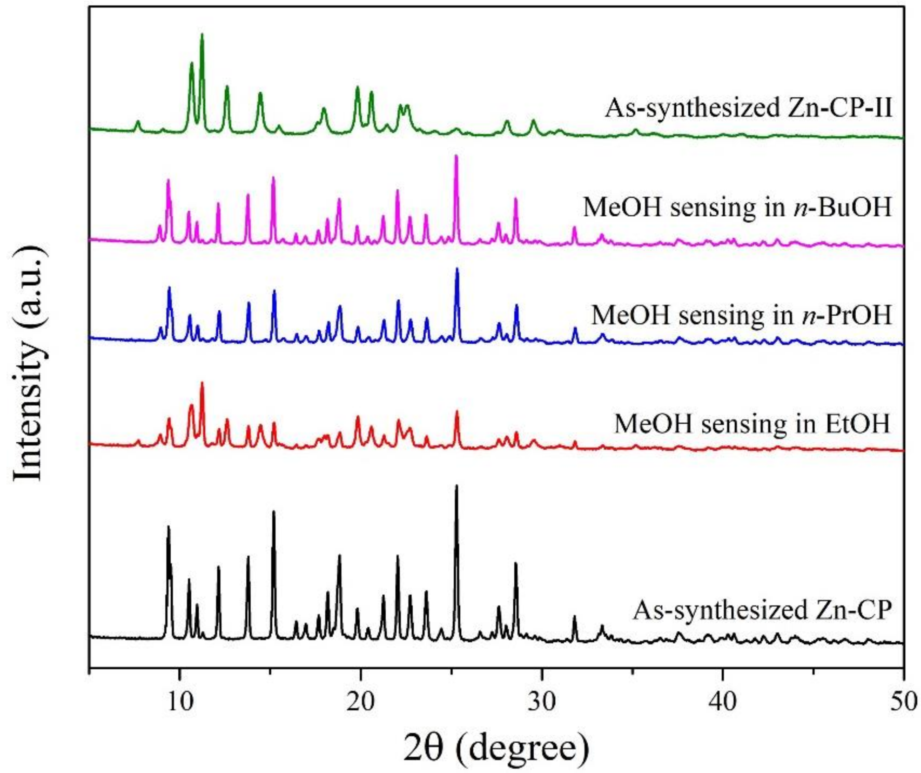

Fig. S20 PXRD patterns of **Zn-CP** before and after methanol sensing in dry ethanol, dry *n*-propanol and dry *n*-butanol, respectively.

Table S1. Kamlet-Taft solvent parameters of the pure solvents[36]

Entry	Solvents	Kamlet-Taft parameters		
		α	β	π*
1	Water	1.17	0.47	1.09
2	ACT	0.00	0.51	0.70
3	ACN	0.19	0.37	0.75
4	DCM	0.13	0.10	0.82
5	DMF	0.00	0.69	0.88
6	DMA	0.00	0.76	0.88
7	EtOAc	0.00	0.45	0.55
8	THF	0.00	0.58	0.55
9	MeOH	0.98	0.66	0.60
10	EtOH	0.86	0.75	0.54
11	n-PrOH	0.84	0.90	0.52
12	n-BuOH	0.84	0.84	0.47
13	n-hexane	0.00	0.00	-0.08
14	Toluene	0.00	0.11	0.54

Note: α = Hydrogen bond donor, β = Hydrogen bond acceptor, π* = polarizability/dipolarity

Table S2. Comparison of solid-state excitation and emission of CPs based on 2,5-Dihydroxyterephthalic (H_4dhtp)

Compounds	Excitation wavelength (nm)	Emission wavelength (nm)	References
$[Zn(L)(Cz\text{-}3,6\text{-}bpy)]_n$	370	522	*Cryst. Growth Des*. **2022**, 22, 228−236
$\{[Cd(4\text{-}bpdh)(L)]\}_n$ $\{[Cd(3\text{-}bpdh)(L)0.5\text{-}(L)_{0.5}(H_2O)]\cdot 2H_2O\}_n$	350	456 462	*Cryst. Growth Des*. **2021**, 21, 6110−6118
SNNU-300	367	439	*J. Solid State Chem*. **2021**, 300, 122212
$\{[Zn_2(H_2L)(L)_{0.5}(azpy)_{0.5}\text{-}(H_2O)]\cdot 4H_2O\}$	390	530	*Chem. Eur. J.* **2012**, 18, 237 – 244
$[\{Cd(bpe)_{1.5}(L)\}]_n$	360	412	*Chem. Eur. J.* **2019**, 25, 12196-12205
$\{[Zn(4\text{-}bpdh)(L)]\cdot(MeOH)(H_2O)\}_n$	350	394	*Chem. Eur. J.* **2016**, 22, 14998 – 15005
$[Cd_2(L)(4,5\text{-}idc)(H_2O)_4]$	360	521	*ACS Appl. Mater. Interfaces* **2020**, 12, 41776−41784
SNNU-301	370	480	*ACS Appl. Mater. Interfaces* **2022**, 14, 55997−56006
Zn-CP	**360**	**-**	***This work***

Table S3. Comparison of the performance of luminescent MOF materials for water sensing

MOF materials	Media	Linear ranges (%v/v)	Detection method	LOD (%v/v)	Ref.
Eu-MOFs/N,S-CDs	EtOH	0.05-4	Shifted-emission and turn-on	0.03	*Anal. Chem*. **2016**, 88, 1748−1752
Mg(DHT)	THF	0-1	ESIPT and Turn-on	-	*Dalton Trans*., **2021**,50, 6901-6912
Tb^{3+}@p-CDs/MOF	EtOH	0-30	Shifted-emission	0.28	*Dalton Trans*., **2017**,46, 7098-7105
$Eu_{0.05}Tb_{0.95}(OBA)(H_2O)Cl$	DMF	0-0.8	Turn-on	0.10	*Dalton Trans*., **2021**,50, 143-150

R6G@Eu-MOF	DMF ACN DMSO THF MeOH EtOH *i*-PrOH *n*-BuOH	0-12.4 0-10 0-4 0-1.8 0-3.5 0-1 0-0.8 0-0.4	Ratiometric	0.085 0.094 0.046 0.032 0.032 0.028 0.016 0.021	*Anal. Chem.* **2020**, 92, 8974−8982
$Eu_{0.02}Dy_{0.18}$-MOF	EtOH	0-0.3	Turn-off	0.1	*Anal. Chem.* **2019**, 91, 3, 2148–2154
SNNU-301	DMSO	0-5.2	ESIPT and Turn-on	0.011	*ACS Appl. Mater. Interfaces* **2022**, 14, 55997−56006
$[Cd_2(4,5\text{-idc})(2,5\text{-tpt})(H_2O)_4]$	DMF	0-50	ESIPT by shifted-emission and turn-off	0.25	*ACS Appl. Mater. Interfaces* **2020**, 12, 41776−41784
Zn-db-3	EtOH MeOH THF	0-15 0-10 0-10	ESIPT and shifted emission	0.05	*J. Mater. Chem. C*, **2022**, 10, 7558–7566
Zn-CP	**MeOH** **EtOH**	**0-12** **0-12**	**ESIPT and shifted emission**	**0.08** **0.08**	**This work**
Zn-CP-II	**MeOH** **EtOH**	**0-20** **1-10**	**ESIPT and turn-on**	**0.05** **0.04**	

Note: DHT= 2,5-dihydroxyterephthalic acid, H_2OBA = 4,4′- oxybisbenzoic acid, R6G = Rhodamine 6G dye, 2,5-tpt = 2,5-dihydroxyterephthalic acid and 4,5-idc = 4,5-imidazoledicarboxylic acid

Table S4. Comparison of luminescence intensity in different alcohol solvents of **Zn-CP** probe

Solvents	**Luminescence intensity (a.u.)**
Methanol	2.62×10^4
Ethanol	6.79×10^3
n-Propanol	1.83×10^3
n-Butanol	1.68×10^3

Table S5. Comparison of the performance of luminescent materials for methanol sensing

MOF materials	Media	Linear ranges (%v/v)	Detection method	LOD (%v/v)	Ref.
MOF-76	Hydrated Ethyl Alcohol Fuel (HEAF)	0.6-5.5	Turn-on	0.82	*J. Rare Earths.*, **2019**, 37, 225-231
NOCDs	real alcoholic beverage	0.125-4	Quenching	0.11	*RSC Adv.*, **2020**, 10, 22522–22532
Zn-MOF	EtOH	0-2.44	Turn-on	0.07	*Dalton Trans.*, **2020**,49, 10240-10249
Zn-CP	EtOH *n*-PrOH *n*-BuOH	5-30 5-25 5-25	Turn-on	0.28 0.52 0.35	**This work**